

## Supplementary content for

### Discovery of effective solvents for platelet-type graphite nanofibers

L. Guardia, J.I. Paredes, S. Villar-Rodil, J.-N. Rouzaud, A. Martínez-Alonso, J.M.D.

Tascón

#### S1. Microscopic characterization of the samples

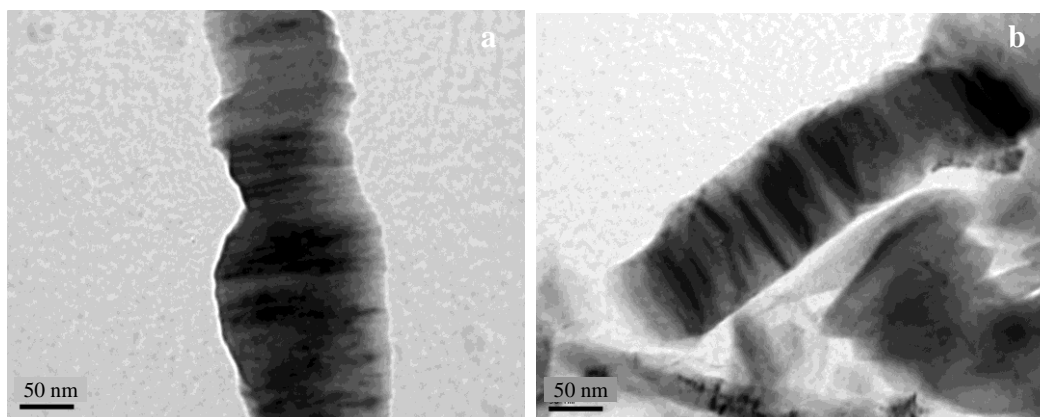


**Figure S1.** TEM images of the as-prepared (a) and heat-treated (b) nanofibers. In both cases, the observed structures are consistent with the idea of graphene layers stacked in the direction of the nanofiber axis.

#### S2. Raman spectra of the samples (including second order region)

Fig. S2 shows Raman spectra for as-prepared (black) and heat-treated (gray) PGNFs. The first order spectrum ( $1100\text{-}1700\text{ cm}^{-1}$ ) is dominated in both cases by bands located at  $\sim 1582\text{ cm}^{-1}$  (G band), which is characteristic of  $\text{sp}^2$ -bonded carbon, and  $\sim 1350\text{ cm}^{-1}$  (D band), which is known to arise as a result of structural disorder in the graphitic lattice (atomic vacancies, edges, etc) [S1,S2]. An additional, weaker band at  $\sim 1620\text{ cm}^{-1}$  (D' band, also defect-related) can be seen as a shoulder on the high frequency side of the G band. The intense defect-related D band for the as-prepared PGNFs ( $I_{\text{D}}/I_{\text{G}} \sim 1.9$ ) must be due to the relatively high fraction of edge carbon atoms present. Indeed, similar  $I_{\text{D}}/I_{\text{G}}$  values have been reported for pristine graphene flakes with lateral dimensions comparable to the widths of these nanofibers (50-200 nm) [S3].

The second-order Raman spectra (i.e., 2300-3300  $\text{cm}^{-1}$  region) display four different bands, that are also characteristic of graphitic materials [S2,S4]. The most relevant one is the 2D peak, located at about 2695  $\text{cm}^{-1}$ , which is the overtone of the D band. Additional, less intense features are observed at 2460  $\text{cm}^{-1}$  ( $G^*$  band, assigned to a combination mode of optical and acoustic phonons), 2950  $\text{cm}^{-1}$  (D+G band, a combination mode of the D and G bands) and 3250  $\text{cm}^{-1}$  ( $2D'$  band, overtone of the  $D'$  band). The  $G^*$  and  $2D'$  peaks are relatively weak but well-defined features in highly ordered graphitic structures, which tend to fade away and/or broaden in the presence of significant amounts of disorder. The D+G band is exclusively induced by defects. The intensity of the 2D peak tends to decrease in the presence of disorder and also analysis of its lineshape reveals information about the three-dimensional stacking order of the sample [S4]. The main differences between the spectra of as-prepared PGNFs and HT-PGNFs in this range were: (i) a higher relative intensity of the bands related to the presence of defects for the as-prepared PGNFs (D+G band) and the opposite (lower relative intensity) for bands related to order ( $G^*$ , 2D,  $2D'$ ) (ii) a narrower, slightly more asymmetric 2D band for the HT-PGNFs, which is indicative of a higher degree of three-dimensional stacking order [S4].

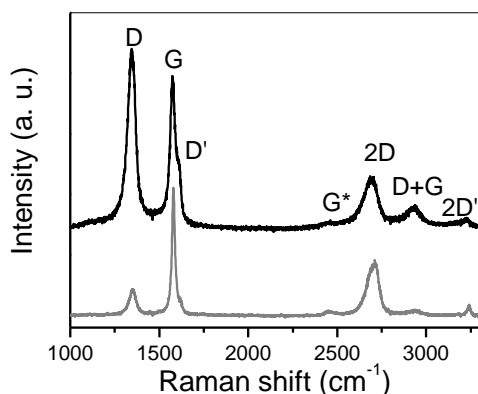


**Figure S2.** First- and second-order Raman spectra for the as-prepared (black) and heat-treated (gray) nanofibers.

### **S3. Estimation of the percentage of edge carbon atoms decorated with oxygen in the as-prepared PGNF surface from the XPS results**

To calculate the percentage of edge carbon atoms on the nanofiber surface that are decorated with oxygen atoms, we assumed that (i) the XPS probing depth is  $\sim 3$  nm [S5],

(ii) the oxygen atoms are only bound to edge carbon atoms, but not to basal plane carbon atoms, and (iii) an edge carbon atom can be bound to just one oxygen atom. With these assumptions, the estimated percentage of edge carbon atoms decorated with oxygen is 60% for armchair edges and 70% for zig-zag edges. Previous work has determined that while zig-zag and armchair edges coexist in this type of nanofiber, the former are dominant [S6], so the actual oxygen coverage should be closer to the value estimated for zig-zag edges (70%).

**Table S1.** Values of surface tension ( $\gamma$ , in  $\text{mJ m}^{-2}$ ), Hildebrand ( $\delta_T$ , in  $\text{MPa}^{1/2}$ ) and Hansen solubility parameters ( $\delta_D$ ,  $\delta_P$  and  $\delta_H$ , in  $\text{MPa}^{1/2}$ ) for different solvents as well as absorbance at 660 nm of PGNF dispersions in these solvents.

Solvents	$\gamma$	$\delta_T$	$\delta_D$	$\delta_P$	$\delta_H$	Absorb. (a.u.)
<i>n</i> -Pentane	16.05	14.50	14.5	0	0,00	0.0014
Diethyl ether	17.06	15.64	14.5	2.9	5,1	0.0095
<i>n</i> -Hexane	18.42	14.90	14.9	0	0	0.0016
Isopropyl alcohol	20.93	23.58	15.8	6.1	16.4	12.8919
Ethanol	22.32	26.52	15.8	8.8	19.4	4.1496
Methanol	22.55	29.61	15.1	12.3	22.3	1.4904
Acetone	23.32	19.94	15.5	10.4	7.0	0.7806
1-Propanol	23.45	24.60	16.0	6.8	17.4	8.1501
1-Butanol	24.67	23.20	16.0	5.7	15.8	16.7731
Allyl alcohol	25.68	25.72	16.2	10.8	16.8	4.4499
<i>o</i> -Dichlorobenzene	26.84	20.47	19.2	6.3	3.3	7.4544
Tetrahydrofuran	27.31	19.46	16.8	5.7	8.0	1.9705

Acetic acid	27.42	21.37	14.5	8.0	13.5	4.4562
Dichloromethane	27.89	20.20	18.2	6.3	6.1	1.9657
Acetonitrile	29.29	24.40	15.3	18.0	6.1	1.5215
o-Xylene	30.04	18.10	17.8	1.0	3.1	0.0060
Nitroethane	32.66	22.73	16.0	15.5	4.5	5.9955
Cyclopentanone	33.87	22.11	17.9	11.9	5.2	4.0824
Cyclohexanol	33.91	22.04	17.4	4.1	13.5	13.4382
<i>N,N</i> -Dimethylformamide	36.76	24.86	17.4	13.7	11.3	0.0884
Nitromethane	37.19	25.08	15.8	18.8	5.1	3.2758
Formic acid	37.58	24.93	14.3	11.9	16.6	0.1669
<i>N</i> -Cyclohexyl-2-pyrrolidone	38.80	20.49	18.2	6.8	6.5	0.4954
<i>N</i> -Methyl-2-pyrrolidone	40.07	22.96	18.0	12.3	7.2	0.0397
Aniline	43.38	22.50	19.4	5.1	10.2	0.1613
$\gamma$ -Butyrolactone	46.50	26.29	19.0	16.6	7.4	1.0695
Formamide	58.35	36.65	17.2	26.2	19.0	0.0006
Water	71.81	47.84	15.6	16.0	42.3	7.2723

## References

[S1] Ferrari AC, Robertson J. Interpretation of Raman spectra of disordered and amorphous carbon. *Phys Rev B* 2000; 61: 14095-107.

[S2] Pimenta MA, Dresselhaus G, Dresselhaus MS, Cañado LG, Jorio A, Saito R. Studying disorder in graphite-based systems by Raman spectroscopy. *Phys Chem Chem Phys* 2007; 9 : 1276-91.

[S3] Green AA, Hersam MC. Solution phase production of graphene with controlled thickness via density differentiation. *Nano Lett* 2009; 9: 4031-6.

[S4] Malard LM, Pimenta MA, Dresselhaus G, Dresselhaus MS. Raman spectroscopy in graphene. *Phys. Rep.* 2009; 473: 51-87.

[S5] Briggs D, Seah MP. *Practical Surface Analysis. Second Edition, Volume 1. Auger and X-ray Photoelectron Spectroscopy*, Chichester :Wiley; 1990.

[S6] Anderson PE. A method for characterization and quantification of platelet graphite nanofiber edge crystal structure. *Carbon* 2006; 44: 2184-90.